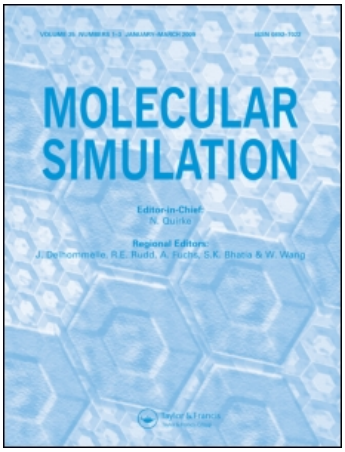


**Molecular Simulation**
Publication details, including instructions for authors and subscription information:
http://www.informaworld.com/smpp/title~content=t713644482

# Numerical Study of the Structural and Thermal Properties of Vitreous Silica

P. Jund[a]; R. Jullien[a]
[a] Laboratoire des Verres - Université Montpellier 2, Montpellier, France

**To cite this Article** Jund, P. and Jullien, R.(2000) 'Numerical Study of the Structural and Thermal Properties of Vitreous Silica', Molecular Simulation, 24: 1, 25 — 49
**To link to this Article: DOI:** 10.1080/08927020008024185
**URL:** http://dx.doi.org/10.1080/08927020008024185

*Molecular Simulation*, 2000, Vol. 24, pp. 25–49
Reprints available directly from the publisher
Photocopying permitted by license only



# NUMERICAL STUDY OF THE STRUCTURAL AND THERMAL PROPERTIES OF VITREOUS SILICA

P. JUND* and R. JULLIEN

*Laboratoire des Verres - Université Montpellier 2, Place E. Bataillon Case 069, 34095 Montpellier France*

*(Received April 1999; accepted June 1999)*



We use classical molecular dynamics simulations to study both the structural modifications through the glass transition and the thermal conductivity $\kappa$ of a model silica glass. The first part is based on the Voronoï tessellation and we show that the structural freezing following upon the glass transition is noticeable in all the geometric characteristics of the Voronoï cells and a possible interpretation in terms of geometrical frustration is proposed.

In the second part we calculate $\kappa$ directly in the simulation box by using the standard equations of heat transport. The calculations have been done between 10 and 1000 Kelvin and the results are in good agreement with the experimental data at temperatures above 20 K. The plateau observed around 10 K can be accounted for by correcting our results taking into account finite size effects in a phenomenological way.

*Keywords:* Numerical simulations; glasses; structure; thermal properties

## I. STRUCTURAL ANALYSIS

### A. Introduction

Silica is a common material which is of great importance in chemistry, geology and industrial applications. It is also a prototype of a network forming glass. All these reasons explain why it has been the topic of a great amount of studies. Nevertheless many features of this typical "strong" glass need still to find a satisfactory explanation. For example the origin of the First Sharp Diffraction Peak (FSDP) is still controversial [1]. The origin

*Corresponding author.

(and the connection to the FSDP) of the so-called Boson peak remains the topic of many studies, both experimental and theoretical [2]. With the development of the computing speed a new type of studies has emerged in the past decade which can be called "computer experiments". Indeed numerical simulations have been used to study the vibrational spectrum [3–6] or the structural characteristics [7–9] of various model silica glasses. Within this framework we present in this paper a classical molecular dynamics study essentially focused on the evolution of the local structure in such a system.

The first step in that kind of endeavor is to choose the interparticle potential: we decided to use the two-body potential proposed by van Beest *et al.* [10]. Indeed a study of the influence of the quenching rate on the properties of amorphous silica has shown that this potential based on *ab initio* parameters gives excellent results compared to experimental data both for the structural characteristics [9] and the vibrational properties [5] of vitreous silica. Similarly to what has been done earlier in the case of high pressure silica samples [11] we combine the molecular dynamics with the Voronoï tessellation scheme in order to have a better insight into the structural evolution of the system during the quenching procedure. We want to know if and how the glass transition leaves a "signature" in the geometrical characteristics of the Voronoï cells. We recall that the Voronoï cell attached to a particle is an extension, for disordered systems, of the Wigner-Seitz cell and gives information on the local structure around this particle.

Our results as a function of temperature show the structural freezing consecutive to the glass transition in all the geometric characteristics of the Voronoï cells. Moreover when extrapolating the high temperature data to lower temperatures, it seems that the system behaves as if it would like to reach locally an ideal underlying structure satisfying the basic energetic requirements imposed by the potential. But, since this structure cannot be developed up to long distances, an amorphous system is obtained instead at low temperature. Therefore we suggest that the structural freezing below $T_g$ is mainly a consequence of this impossibility, also called "geometrical frustration" [12].

## B. Simulations

If one wants to perform realistic simulations on silica glasses the major point is to choose an interaction potential which gives reasonable results compared to experimental data. Several choices are today possible, but in the last years one of the most successful classical potentials is the so-called BKS potential developed by van Beest *et al.* [10]. Though designed originally from the

crystalline phases of silica, it has been shown that it also describes very well the structural [9] and vibrational [5] properties of amorphous silica.

The functional form of the pairwise BKS interaction between two particles $i$ and $j$ is given by

$$U(r_{ij}) = \frac{q_i q_j e^2}{r_{ij}} + A_{ij} \exp(-B_{ij} r_{ij}) - \frac{C_{ij}}{r_{ij}^6} \tag{1}$$

where $r_{ij}$ is the interparticle distance, $e$ the charge of an electron and the parameters $A_{ij}$, $B_{ij}$ and $C_{ij}$ are fixed as follows: $A_{SiO} = 18003.7572$ and $A_{OO} = 1388.773\,\text{eV}$; $B_{SiO} = 4.87318$ and $B_{OO} = 2.76\,\text{Å}^{-1}$; $C_{SiO} = 133.5381$ and $C_{OO} = 175.0\,\text{eV Å}^6$. Note that except for the Coulomb interaction ($q_{Si} = 2.4$ and $q_O = -1.2$) there is no interaction between Si atoms.

This original form contains an unphysical property at short distances since it diverges to minus infinity. To overcome this drawback which is especially annoying at high temperature, we have added a short range repulsive term ($\sim 1/r_{ij}^{40}$) which insures that the potential goes to infinity at small interatomic distances and is practically equivalent to the original potential for $r_{ij} \geq 1.2$ Å (Si—O interaction), and $r_{ij} \geq 1.6$ Å (O—O interaction) without introducing any artificial energy barrier.

The Coulomb interactions were computed using the Ewald summation method [13] with a characteristic constant $\kappa = 6.5/L$, where $L$ is the cubic box size, and considering 501 $k$-vectors in reciprocal space ($|k| \leq 6 \times 2\pi/L$). These values insure that the potential energy is obtained with a relative error smaller than $5 \times 10^{-4}\%$. No cut-off was used for the pairwise interaction.

We performed molecular dynamics simulations for microcanonical systems containing 216 silicon and 432 oxygen atoms confined in a cubic box of edge length $L = 21.48$ Å, which corresponds to a mass density of $\approx 2.18\,\text{g/cm}^3$ very close to the experimental value of $2.2\,\text{g/cm}^3$. Periodic boundary conditions were used to limit surface effects. In order to insure energy conservation even at high temperature a timestep of 0.7 fs was necessary. This value is substantially lower than the one used in previous studies (1.6 fs [9] or 1.0 fs [5]) which may be due to our "conservative" potential correction. The 4-th order Runge–Kutta algorithm was used to integrate the equations of motion. The glass configurations were obtained by quenching well equilibrated initial liquid samples obtained by melting $\beta$-cristobalite crystals at a temperature around 7000 K. After full equilibration of the liquid ($\approx 40000$ timesteps), the system was cooled to zero temperature at a quench rate of $2.3 \times 10^{14}\,\text{K/s}$ which was obtained by removing the corresponding amount of energy from the total energy of the system at each iteration. Due to computer time

limitations this cooling rate is rather fast but it has the advantage compared to other procedures involving either stepwise cooling [9] or temperature dependent rates [5] to be linear and continuous all along the quenching procedure. At several temperatures during the quenching process the configurations (positions and velocities) were saved. Each configuration was used to start a constant-energy molecular dynamics calculation during which the temperature was recorded as a function of time. The temperature was in all cases remarkably stable and only slight relaxation effects could be observed. Nevertheless to avoid transient configurations we allowed for each temperature and for each sample, 10000 relaxation steps followed by 50000 supplemental time steps (for a total simulation time of 42 ps) during which all the calculations were done. Apart from the calculation of standard quantities (radial pair distribution function, mean square displacement) we included also in our molecular dynamics code a Voronoï tessellation scheme similar to the one that we have developed for monocomponent soft-sphere glasses [14]. This scheme has been modified to take into account several types of atoms and thus it permits to follow the local structure around the silicon atoms and the oxygen atoms as a function of temperature during the quenching procedure. Here the Voronoï cell is always defined as being the region of space closer to a given atom center than to any other and no dissymetry between the two components has been introduced as it is the case in the "navigation map" procedure [15]. The Voronoï cell characteristics as well as all the other quantities have been averaged over samples obtained from 5 independent starting configurations in order to improve the statistics of the results. The whole simulation lasted for more than 3 million timesteps which were run on 4 nodes of an IBM/SP2 parallel computer.



### C. Results

As said earlier this potential has already been used in other studies of amorphous silica and since we did not modify the BKS parameters our results concerning the radial pair distribution [5, 9] or the diffusion constant [6] are exactly identical to the referenced results and therefore we do not come back to these standard results here. Our aim is to localize the glass transition temperature $T_g$ through the study of the structural characteristics (*via* the Voronoï tessellation) of our model silica system. Nevertheless a straightforward way of determining $T_g$ is to monitor the potential energy *versus* the temperature, as has already been done for another model silica glass [7]. The evolution of the average potential energy per particle *versus* the temperature is shown in Figure 1.

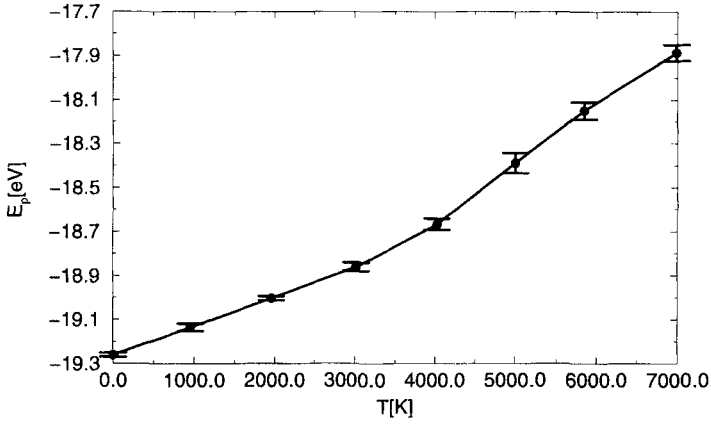


FIGURE 1 Average potential energy per particle as a function of temperature.



With increasing temperature, the potential energy as well as the standard deviation increases as expected. Nevertheless one can observe an acceleration of this increase between 3000 and 4000 K, corresponding to the passage from a solid to a liquid behavior. Due to the fast cooling rate the value of $T_g$ is much higher than the experimental value (1446 K) but it is coherent with the value of $\approx 3500$ K obtained from the fit of $T_g$ *versus* the quenching rate proposed by Vollmayr *et al.* [9]. Note that we observe a non negligible increase of the potential energy in the glass phase contrarily to what was obtained by Della Valle *et al.* [7], (Fig. 3) who used a direct minimization procedure after the quench to investigate the "inherent structures" [16]. Here we let the system evolve freely after the quench and it seems that even at low temperatures structural relaxation occurs.

Once we know approximately the value of $T_g$ (to our purpose this level of accuracy is sufficient) we can tackle the study of the geometrical characteristics of the Voronoï cells in order to follow the local structure as a function of temperature. All the characteristics of the cells have been obtained (surface, number of faces, number of edges, *etc.*..) but we want to discuss here only some representative quantities. The first one is the variation of the volume of the Voronoï cells. This variation is represented in Figure 2 for the silicon (a) and the oxygen (b) atoms together with the corresponding standard deviations (c). With decreasing temperature the volume of the silicon cell decreases while the volume of the oxygen cell increases (these opposite variations are a consequence of our constant-volume calculations). Again a change of behavior is visible and corresponds to a slowing down of the evolution below the glass transition temperature.

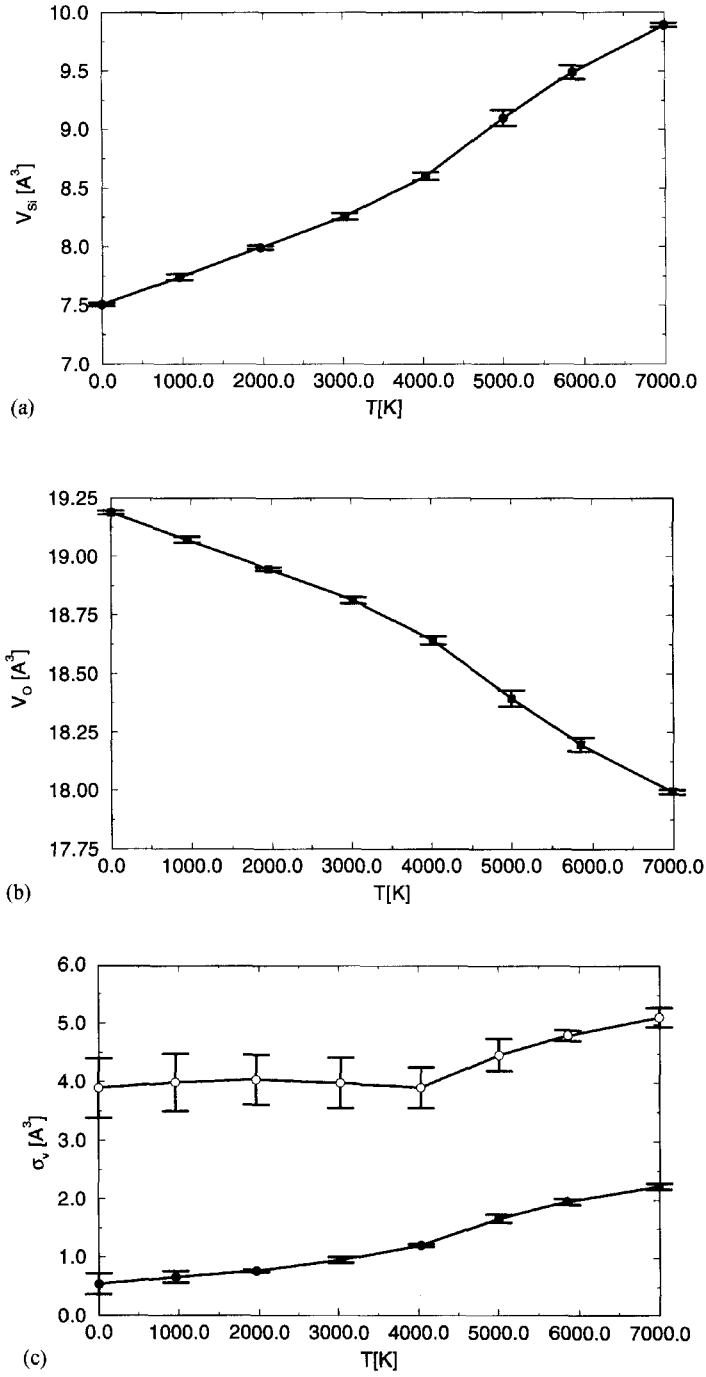


FIGURE 2 Variation of the cell volume *versus* temperature: (a) silicon; (b) oxygen; (c) Standard deviation $\sigma_V$ *versus* temperature: •: silicon; ○: oxygen.

An even more striking behavior is observed in Figure 2c where the standard deviation $\sigma_V$ is plotted as a function of temperature. This is a quantity of physical interest since it measures the local density fluctuations around the particles. For both types of atoms, $\sigma_V$ decreases with decreasing temperature as if it would like to tend to zero at $T = 0\,\mathrm{K}$ but then below 4000 K this trend is stopped and finally $\sigma_V$ saturates around non-zero values characteristic of spatial disorder. This is a direct observation of the low-temperature saturation of the density fluctuations which is a signature of the glass transition. Even though not reported here, exactly the same behavior can be observed for the evolution of the surface of the Voronoï cells as a function of temperature.

To investigate further the structural evolution during the quench, we looked at the angle distributions. First we studied the tetrahedral O—Si—O angle which should be ideally equal to 109°.47 in a perfect tetrahedron. As can be seen in Figure 3a, this angle varies between 110°.5 at low temperature and 117° at 7000 K, with a slight change of behavior around $T_g$.

The same behavior is observed for the corresponding standard deviation (Fig. 3c full circles) which is quite small and decreases when $T$ decreases. This shows firstly that with increasing temperature the $SiO_4$ tetrahedra survive even in the liquid phase but become more and more distorted and secondly that the glass transition does not strongly affect the local environment around the silicon atoms.

On the contrary the glass transition is more clearly visible in the angle Si—O—Si, which measures the relative position and orientation of two

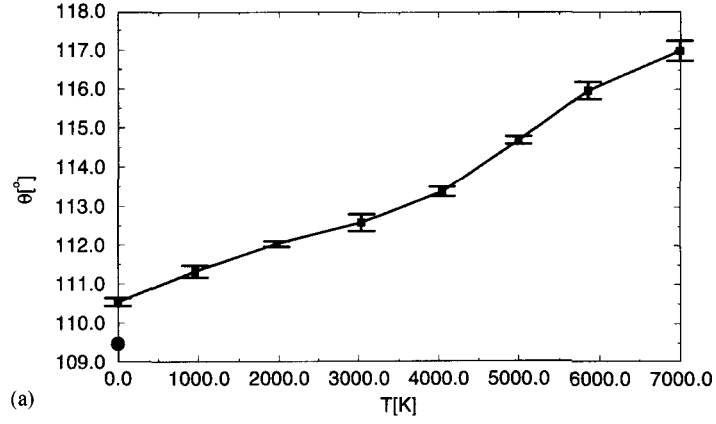


FIGURE 3 Variation as a function of temperature of: (a) $\theta$, the O—Si—O angle; (b) $\phi$, the Si—O—Si angle; (c) the standard deviations $\sigma_\theta$ and $\sigma_\phi$ *versus* temperature: •: silicon; ○: oxygen.

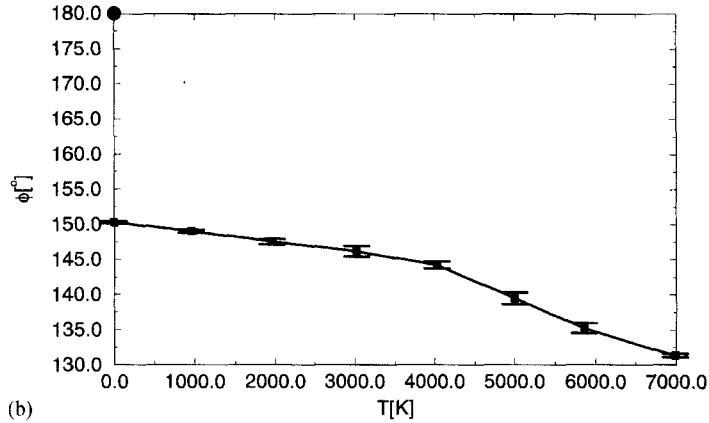


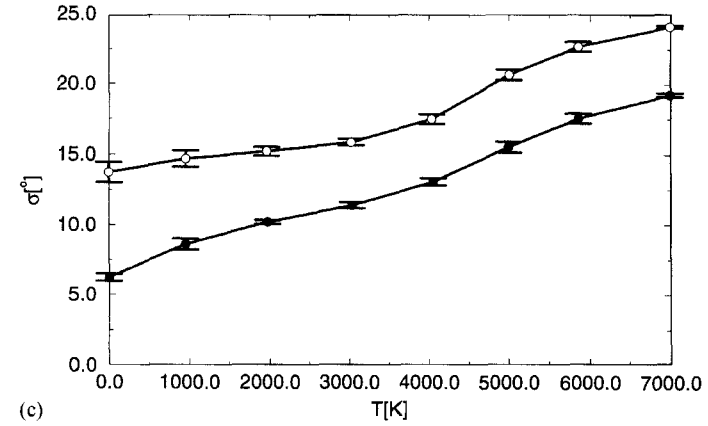


FIGURE 3 (Continued).

neighboring $SiO_4$ tetrahedra, as can be seen in Figure 3b. With decreasing temperature within the liquid phase, the Si—O—Si angle increases and seems to converge towards 180° (a least square quadratic fit of the four points in the liquid phase gives an extrapolated value of 175°), but again below 4000 K this decrease slows down and finally the angle converges towards a value close to 150°, a value coherent with previous simulations [5, 9], but slightly higher than the value 144° found in X-ray diffraction experiments [17]. The decrease of this angle is coherent with the views of a densifying network with increasing temperature this densification taking place around the oxygen atoms. Also since it measures the relative orientation between two neighboring tetrahedra, this decrease corresponds to a decrease of the effective volume of the oxygen atoms with increasing

temperature and since we work at constant volume it implies an expansion of the silicon volume, which is indeed the behavior observed in Figure 2. Concerning the standard deviation of the Si—O—Si angle represented in Figure 3c (open circles) it increases rapidly in the liquid phase (above 4000 K) while in the glass phase this increase is more slow. This again is an illustration of the structural freezing below $T_g$.

Another quantity which reflects the glass transition is the effective coordination number, $z$, which is in fact the average number of faces of the Voronoï cells. This quantity should be considered with some care since, generally, it does not correspond to the true "chemical" coordination number. To give an example, in $\beta$-cristobalite the Voronoï cell of the silicon atoms is a tetrahedron ($z = 4$) while the Voronoï cell of the oxygen atoms is the polyhedron represented in Figure 4 with $z = 8$. In the Voronoï "sense" the nearest neighbors of an oxygen atom in $\beta$-cristobalite are two silicon atoms (represented by the triangular faces in Fig. 4), and six oxygen neighbors (represented by the pentagonal faces in Fig. 4). In fact, such a cell is highly "degenerate": an infinitely small random perturbation of the atomic positions ($\approx 10^{-2}$ Å) is sufficient to create new extra-small triangular faces and the coordination number of the oxygen atoms flips to $z \approx 19.7$ while the coordination of the silicon atoms remains close to 4. This could be avoided by doing a smoothed Voronoï tessellation which excludes small



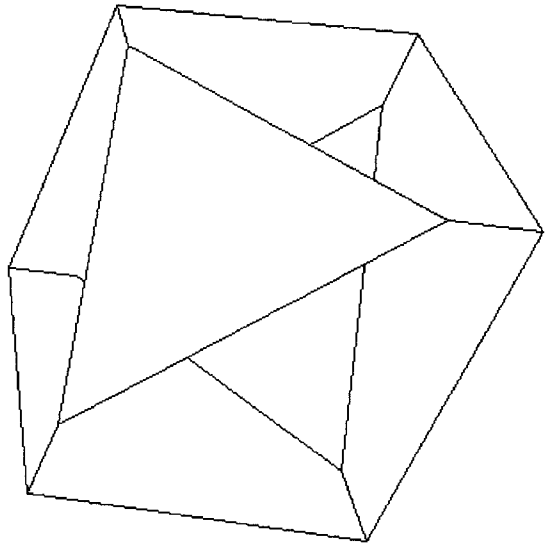

FIGURE 4 The Voronoï cell of an oxygen atom in $\beta$-cristobalite.

faces with an area smaller than 10% of the largest cell face [11] but we have rather chosen not to use this technique and analyze raw data. The variation of $z$ as a function of temperature is represented in Figure 5a for the silicon atoms and Figure 5b for the oxygen atoms.

The glass transition can again clearly be identified: for the silicon atoms, $z$ increases with increasing temperature with a slope that is more important above 4000 K. For the oxygen atoms, $z$ is approximately constant in the glass phase and then decreases for temperatures above $T_g$. It should be noted that the relative variation of $z$ between 0 and 7000 K is small, especially for the oxygen atoms. In the liquid phase, with decreasing temperature, the local structure around the silicon atoms evolves towards a

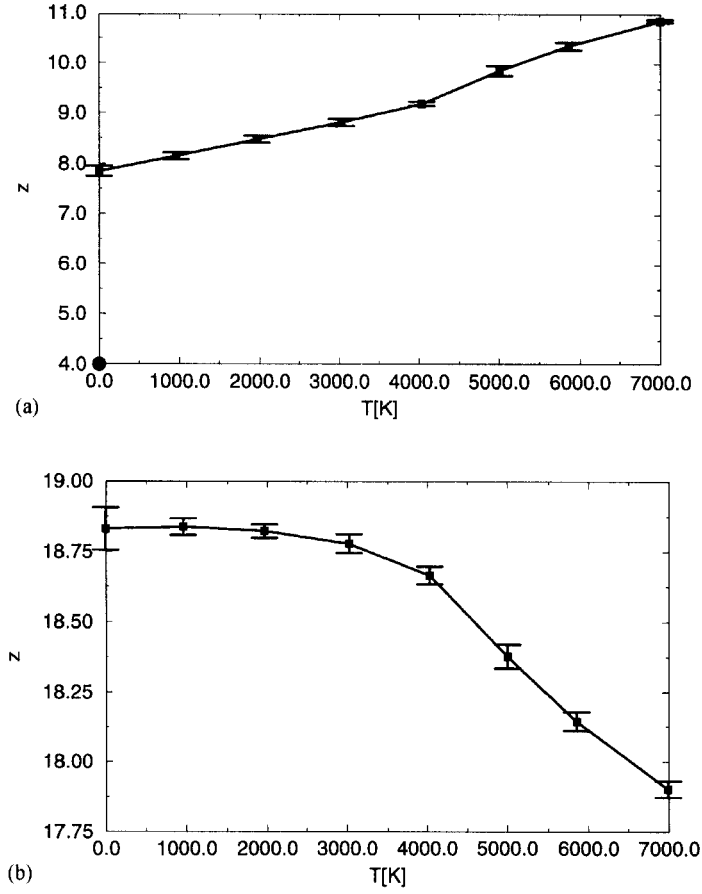


FIGURE 5 Variation of the effective coordination, $z$, as a function of temperature: (a) silicon atoms; (b) oxygen atoms.

perfect tetrahedral arrangement ($z = 4$) and then converges to a value higher than 4 in the glass phase due again to the structural freezing below $T_g$.

### D. Discussion

All these results can be discussed in the light of the conclusions drawn for the analogous geometrical analysis performed in a monoatomic soft-sphere glass [14]. In that case, the system tries to reach an icosahedral arrangement (with dodecahedral Voronoï cells) when the temperature is lowered down from the liquid phase, but, since such an arrangement can not be realized at large distances in the regular three-dimensional space, the system gets frozen in a glass phase below a characteristic glass temperature. Such geometrical frustration effects were in that case the consequence of the degeneracy between the face-centered-cubic (FCC) and the hexagonal-close-packed (HCP) structures [12].

Since all the standard deviations presented here seem to go to zero with decreasing temperature, when extrapolated from the liquid phase, it is reasonable to assume that in the case of silica also a $T = 0$ unreachable ideal local structure exists. It is also reasonable to assume that such an ideal arrangement corresponds to a perfect tetrahedral order for the four oxygens bounded to a given silicon atom, as it is for almost all of the known crystalline structures of silica. This assumption is supported by the behavior of $z$, which tries to extrapolate to 4 when $T$ is lowered from the liquid phase, and it is not incompatible with our results for the variation of the angle O—Si—O with temperature (see Fig. 3a). Even if this angle does not show a major change of behavior at $T_g$, an extrapolated value of 109°.47 at $T = 0$ is not inconsistent with the reported data above $T_g$. Moreover, since the angle Si—O—Si seems to extrapolate to 180°, one can imagine that the ideal structure is made of tetrahedral units, like the $sp_3$ coordination of carbon where the silicon atoms would be located at the carbon places and oxygen atoms located in the middle of the C—C bonds (see Fig. 6a). Indeed the tendency to build such a local structure should result from the form of the potential. In particular the tetrahedral arrangement of the oxygens around a silicon atom results from a combination of the Si—O attraction and the repulsion between the oxygens. The tendency to align the Si—O—Si bridges between neighboring tetrahedra is more subtle however, since the long range nature of the ionic part of the potential certainly plays a role.

It is interesting to notice that, among all the known crystalline structures of silica, two particular structures (at least) fully satisfy these criteria,

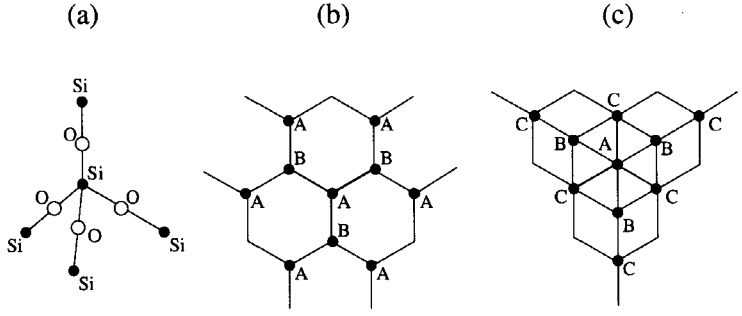


FIGURE 6 The ideal tetrahedral unit around a silicon atom (a) is shown together with the trydimite (b) and $\beta$-cristobalite (c) structures viewed from the top. In (b) and (c) two successive layers connected to a single top unit are represented (the positions of the oxygen atoms have been omitted).

namely the $\beta$-cristobalite and the tridymite structures. In these two structures the above defined tetrahedral units are stacked with sequences ABABAB... (Fig. 6b) and ABCABC... (Fig. 6c), respectively, like in FCC and HCP structures. In fact these structures can be simply built from FCC and HCP structures, by adding to the original structure another one shifted by a fourth of the diagonal of the cubic cell (in the FCC case) and by 3/8 of the $c$-axis of the hexagonal cell (in the HCP case). They correspond respectively to the diamond and wurtzite structures of carbon. When these two structures are considered with the same density, they have exactly the same Si—O distance $d_{SiO}$, and therefore, in the two cases the Voronoï cells for the silicon atoms are regular tetrahedra with the same volume $V_{Si} = \sqrt{3}d_{SiO}^3$. The volume of the oxygen cells, $V_O$, is also the same and therefore the two structures are characterized by the same Si/O volume ratio $R = V_{Si}/(2V_O) = 9/55 = 0.164$, independent on the density. In Figure 7 we have plotted $R = V_{Si}/(2V_O)$ as a function of $T$, as calculated from our simulations, and reported the value $R = 0.164$ at $T = 0$ (open circle). When decreasing the temperature from the liquid phase $R$ decreases as if it would like to reach a value quite close to (or even lower than) 0.164. Therefore, one can interpret the glass transition as a result of local frustration effects. Indeed the system tries to establish a local order similar to the one of tridymite or cristobalite, but these two structures are different, and therefore, due to spatial incompatibilities, no long range order can be generated. But let us pursue this analysis a little bit further, like it has been done for soft sphere glasses or hard sphere packings [14, 18]. Similarly to these model systems, the frustration can be resolved by considering a curved space with positive curvature, namely the sphere $S_3$ [12]. Consider a regular tetrahedron with a silicon atom in the middle and oxygen atoms at the

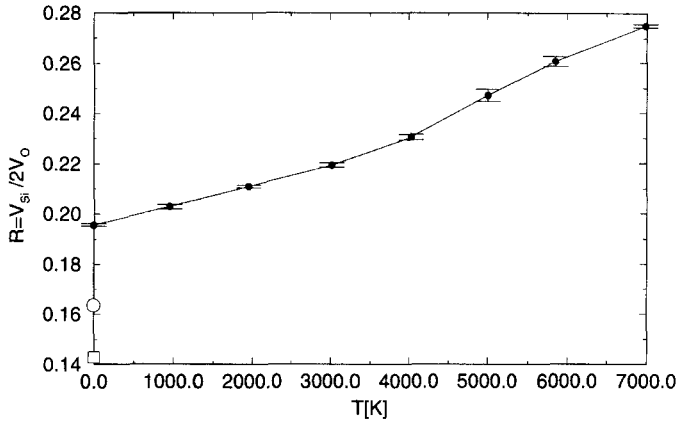


FIGURE 7 Variation of $R = V_{Si}/2V_O$ as a function of temperature. ○: value of $R$ obtained in tridymite or $\beta$-cristobalite; □: value of $R$ obtained in the ideal structure built on $S_3$.



centers of the faces. This tetrahedral unit contains one silica molecule. One can exactly tile an $S_3$ space with 600 tetrahedra like this, and the resulting $SiO_2$ structure (which contains 600 silicons and 1200 oxygens) satisfies all the local requirements defined above. The 120 vertices of the unit tetrahedra are located on the so-called {3, 3, 5} polytope [12]. A good approximation of the ratio $R$ for this structure can be obtained by considering the tetrahedron unit in the regular three dimensional space: the silicon Voronoï cell, limited by the bisector planes of the Si—O bonds, is a tetrahedron of volume 1/8 of the volume of the unit. Therefore the remaining volume for the two oxygen atoms is 7/8 and consequently $R = 1/7 = 0.143$. This value is represented by the open square in Figure 7. It appears that this value corresponds to a better extrapolation of the four points above 4000 K than the one obtained from tridymite or cristobalite (the second order fit of the four liquid points leads to a value of 0.136). Therefore one is tempted to conclude as in the soft sphere case [14]: when lowering the temperature from the liquid phase the system evolves as if it would try to build locally such an ideal structure, but since this structure cannot be realized in the regular three dimensional space, the systems gets frozen in a glassy state below $T_g$. Obviously, the above interpretation should be considered as a suggestion which needs to be confirmed or invalidated by many more calculations that we intend to perform in the future.

## E. Conclusions

With the use of classical molecular dynamics simulations combined with the Voronoï tessellation we have studied in this first part the evolution of the

local structure around the particles of a model silica glass as a function of temperature. The glass transition temperature, $T_g$, obtained from the variation of the potential energy *versus* the temperature is coherent with the value expected for systems quenched at $2.3 \times 10^{14}$ K/s. This transition is clearly visible in the evolution of all the geometric characteristics of the Voronoï cells. The study of the local density fluctuations clearly demonstrates the saturation of these fluctuations below $T_g$ which is the usual signature of the glass transition. The study of the tetrahedral O—Si—O angle shows that with increasing temperature the $SiO_4$ tetrahedra survive but become more and more distorted. The variation of the angle Si —O—Si between two cornersharing tetrahedra is coherent with the views of a densifying network with increasing temperature, this densification happening around the oxygen atoms, while a volume expansion occurs around the silicon particles since we are considering microcanonical ensembles. The different geometric characteristics and in particular the average coordination number evolve with decreasing temperature as if the system would like to reach an ideal structure at $T = 0$, which cannot be realized due to geometrical frustration. This evolution is frozen below the glass transition temperature, and finally the system converges towards an amorphous structure. Our results show that the use of the Voronoï cell characteristics gives not only useful informations on the local structure but can also be used to determine the glass transition unambiguously. This means that even if nothing *dramatic* happens at the glass transition concerning the local structure, *something* happens, which is basically a dynamic freezing of the natural evolution of the structure towards an unreachable ideal structure. Of course we are far away from the timescales used in experiment, but this study, together with others, permits to investigate what happens on the microscopic level in an attempt to explain what is observed at the macroscopic level. (This work has been published originally in Phil. Mag. A 79, 223 (1999).)



## II. THERMAL CONDUCTIVITY

### A. Introduction

The thermal properties of glasses exhibit some specific and unusual features which are well known for quite some time [19]. These features are apparent in the specific heat and the thermal conductivity but we would like to focus here on the thermal conductivity $\kappa$. The temperature dependence of $\kappa(T)$

can be separated in 3 distinct temperature domains:

- At very low temperature ($T \leq 1\,\mathrm{K}$) the thermal conductivity increases like $T^2$. This increase can be explained within the tunneling model [20] which has been proposed almost thirty years ago.
- At intermediate temperatures ($2 \leq T \leq 20\,\mathrm{K}$) the thermal conductivity exhibits a "plateau" for which several explanations have been given [21]. An extension of the tunneling model, the soft-potential model, has been proposed and gives a coherent description of the plateau by introducing the concept of "soft vibrations" [22].
- At high temperature, ($T \geq 30\,\mathrm{K}$), $\kappa(T)$ rises smoothly and seems to saturate to a limiting value $\kappa_\infty$ unlike crystals where $\kappa(T) \sim 1/T$ at elevated temperature. Recently this second rise of the thermal conductivity has also been explained within the soft-potential model [23] which appears to be able to account for all the thermal anomalies of glasses over the whole temperature range.



Our aim here is not to propose a new or alternative explanation of the above mentioned anomalies. The purpose is to perform a molecular dynamics (MD) simulation on a model silica glass using the very widely used BKS potential without any pre-conception of the model able to explain the thermal anomalies of silica. This means that we do not add or inject an *a priori* quantity in the potential to reproduce a specific model. We use the standard definition of the heat transport coefficients that we calculate directly in our simulation box. In fact we introduce artificially inside the system a "hot" and a "cold" plate which therefore induce a heat flux. This flux creates a temperature gradient and once the steady state has been reached we can determine the thermal conductivity. By using plates compatible with the periodic boundary conditions we are able to calculate the thermal conductivity directly during the simulations without any additional parameter. This technique has been inspired by earlier studies [24] in which the plates were treated like hard walls and has mainly been applied to the calculation of the thermal conductivity in 1- or 2-dimensional systems [25, 26]. Nevertheless very recently Oligschleger and Schön applied the same method in a study of heat transport phenomena in crystalline and glassy samples (mainly selenium) [27]. In parallel to these studies which can be called *in situ*, other methods relying on the use of the density and heat flux correlation functions [28] or on the Kubo and Greenwood-Kubo formalism [29] have been developed in order to determine the thermal conductivity of solids. Our results for the thermal conductivity obtained with the BKS potential compare reasonably well with the experimental data. First of all

the order of magnitude is correct above 20 K and, at least in the range 20 K – 400 K, a nice quantitative agreement is obtained. Furthermore, by taking care of finite-size corrections in a very simple phenomenological way, we are able to reproduce the plateau around 10 K. Of course, the very low temperature $T^2$ behavior, which is known to be due to quantum effects, is out of the scope of such a classical calculation.

### B. Modus Operandi

Except the determination of $\kappa(T)$, the simulations are standard classical MD calculations on a microcanonical ensemble of 648 particles (216 $SiO_2$ molecules) interacting *via* the BKS potential described earlier. As in the first study the particles are packed in a cubic box of edge length $L = 21.48$ Å (the density is approximately equal to 2.18 g/cm$^3$) on which periodic boundary conditions are applied to simulate a macroscopic sample. The equations of motion are integrated using a fourth order Runge–Kutta algorithm with a time step $\Delta t$ equal to 0.7 fs. The glassy samples are obtained following the quenching procedure described earlier.

The principle of the thermal conductivity determination is illustrated in Figure 8.

We consider two plates $P_-$ and $P_+$ perpendicular to the $Ox$ axis and located at $x = -L/4$ and $x = +L/4$. These plates have a width $2\delta$ along $Ox$ and their surface is $L^2$. The positions of these plates permit to keep the periodic boundary conditions without introducing an asymmetry in the system. This has the advantage, compared to other studies [30] in which the introduction of the thermostatic plates breaks the symmetry, to use a relatively small number of particles. At each iteration the particles which are

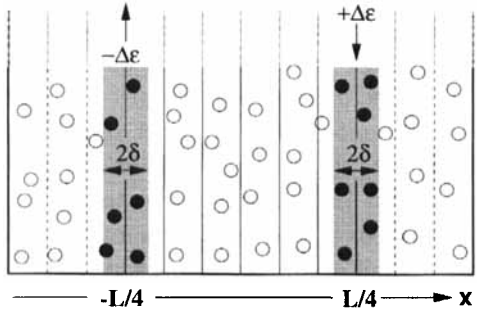


FIGURE 8 Schematic representation of the method used to determine the thermal conductivity. More details can be found in the text.

inside $P_-$ and $P_+$ are determined and their number is respectively $N_-$ and $N_+$. Once these particles are determined a constant energy $\Delta\varepsilon$ is subtracted from the energy of the particles inside $P_-$ and added to the energy of the particles in $P_+$. By imposing the heat transfer in this manner we insure a constant heat flux per unit area $J_x$ [31] which is equal to $\Delta\varepsilon/(2L^2\Delta t)$. (The factor 2 comes from the fact that the heat flux coming from the hot plate splits equally into two parts to reach the cold plate). The energy modification is done by rescaling the velocities of the particles inside the plates. Nevertheless to avoid an artificial drift of the kinetic energy this has to be done with the total momentum of the plates being conserved. For a particle $i$ inside $P_-$ or $P_+$ the modified velocity is given at each iteration by

$$\vec{v}_i' = \vec{v}_G + \alpha(\vec{v}_i - \vec{v}_G) \tag{2}$$

where $\vec{v}_G$ is the velocity of the center of mass of the ensemble of particles in the plate and

$$\alpha = \sqrt{1 \pm \frac{\Delta\varepsilon}{E_c^R}} \tag{3}$$

depending on whether the particles are inside $P_+$ or $P_-$. The relative kinetic energy $E_c^R$ is given by

$$E_c^R = \frac{1}{2}\sum_i m_i \vec{v}_i^2 - \frac{1}{2}\sum_i m_i \vec{v}_G^2 \tag{4}$$

Following the standard definition of the transport coefficients [31] the thermal conductivity is given by

$$\kappa = -\frac{J_x}{\partial T/\partial x} \tag{5}$$

where $\partial T/\partial x$ is the temperature gradient along $Ox$. This formula, known as the Fourier's law of heat flow, is only valid when a stable, linear temperature profile is obtained in the system. To calculate the gradient we divide the simulation box into $N_s$ "slices" along $Ox$ in which the temperature is calculated at each iteration. Due to the periodic boundary conditions we can concentrate only on the $N_s/2$ slices between $x = -L/4$ and $x = L/4$ and have a better determination of the temperature in these slices since by symmetry arguments these slices are equivalent to the $N_s/2$ slices located outside $[-L/4, L/4]$. We can therefore determine the temperature $T_i (i = 1, \ldots, N_s/2)$ of

each slice at each iteration. By averaging each $T_i$ over a large number of iterations to kill the unavoidable large temperature fluctuations (due to the small average number of particles in each slice), we are able to determine after which simulation time $\tau$ the averaged profile of $T(x)$ can reasonably well be approximated by a straight line. After that time we estimate $T(x)$ using a first order least square fit of the averaged $T_i$'s, the slope of which will give us the temperature gradient. At that point all the quantities necessary to calculate $\kappa$ are determined.

Concerning the "practical details" of the simulation we have checked that the results are independent on the choice of $\Delta\varepsilon$ and for the other quantities we have used a compromise between computer time and accuracy of the results. Here are the values used in our simulations: the width of the plates has been taken equal to $2\delta = 1$ Å which means that approximately 30–40 atoms are inside the plates at each iteration. The temperature gradient has been determined on $N_s/2 = 6$ slices, each slice containing approximately 100 particles. $\kappa$ has been determined on samples which have been saved all along the quenching procedure and therefore have different temperatures $T$. To have the same treatment for each sample we have fixed $\Delta\varepsilon$ to 1% of $k_B T$ which appears to be a good choice. The temperature gradients obtained this way are small enough to insure the validity of Eq. (5). The most problematic choice is the simulation time $\tau$. Indeed in order to reach the steady state one needs long MD runs. For us a typical run consists of 50000 MD steps (35 ps) directly after the quench during which the average temperature is fixed and the heat transfer is switched on. Then we perform 450000 supplemental steps (315 ps) with only the heat transfer but no other constraints during which the results are collected and averaged. After this time the temperature gradient should have converged and the value of $\kappa$ should be constant. As we can see in Figure 9, this can be considered to be qualitatively true for the samples above 10 K but certainly not for the low temperature systems.

In fact at low temperature longer runs (1 million steps (700 ps)) are necessary and still the convergence is not perfect (it is interesting to note that though our method converges slowly, it still converges faster than the calculation of $\kappa(t)$ given by a steady state experiment without a temperature gradient ([13], p. 61)). It is also worth noticing that the characteristic sigmoidal shape of the temperature profile observed at 1 K is consistent to what is expected in the intermediate regime where only heat transport over a small distance close to the plates is effective. In the following, only the results above 8 K will be reported.

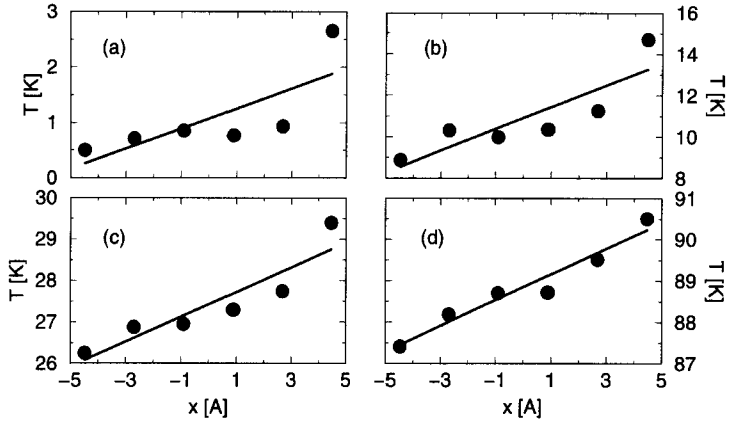


FIGURE 9 Values of the temperature as a function of $x$ in the slices located between $x = -L/4$ and $x = L/4$ for 4 different samples and the corresponding least square linear fit: (a) $T \approx 1$ K; (b) $T \approx 11$ K; (c) $T \approx 27$ K and (d) $T \approx 89$ K.



## C. Results

The results obtained for the thermal conductivity as a function of temperature in our model silica glass are reproduced in Figure 10 and compared to experimental data collected between 1 and 100 K [32] and up to 1000 K [33]. The first observation is that our simulations with the BKS potential give the correct order of magnitude over the whole temperature range (except at very low temperatures) with no adjustable parameters apart from the "technical parameters" described above and the constitutive potential parameters. At very high temperatures, say above 500 K, one observes a more marked saturation of $\kappa(T)$ than in the experiments. This might be explained by the fact that other contributions than the one described here can occur in the experiments at such high temperatures. It is known that the radiative contributions (photon transport) in particular increase quickly in this temperature range and can become of the order of the phonon contributions [33]. In a large intermediate range, 20 K to 400 K, the agreement between the calculated and experimental values is very good. Indeed in the simulation also $\kappa$ increases in this temperature range unlike what is found in crystalline samples. The major discrepancy between the simulation and the experiment can be seen between 8 and 20 K since we do not find the characteristic plateau in the thermal conductivity. In the following, we would like to argue that this discrepancy is essentially due to finite size effects.

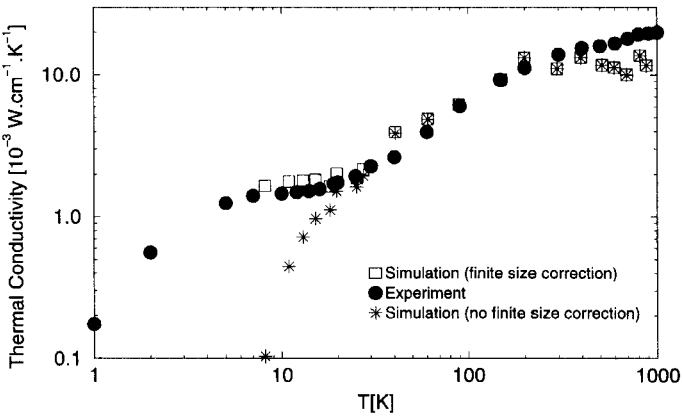


FIGURE 10 Log–log plot of the thermal conductivity as a function of temperature in silica: •: experiment; ∗: simulations; □: simulations with finite-size corrections.



In our cubic finite simulation box with periodic boundary conditions, the components of the $\vec{k}$ wavevectors take discrete values of the form $k_x = n_x 2\pi/L$, where $n_x$ is a relative integer (and similarly for the other space directions), and one cannot find, in principle, propagative phonons with a frequency smaller than a lower cut-off $\omega_c$ which can be estimated by $2\pi v_T/L$, where $v_T$ is the transverse sound velocity. Considering the experimental value $v_T = 3.75 \times 10^5$ cm/s for silica [34] this gives $\omega_c/2\pi \simeq 1.5$ THz (in practice, when diagonalizing the dynamical matrix in our low temperature sample, we find, similarly to a previous work done on the same system [4], a slightly lower first non-zero frequency $\omega_o/2\pi \simeq 1.2$ THz, in agreement with the existence of an excess of modes (maybe non-propagative), the so-called Boson peak [35], in this frequency range [36]. Therefore using the correspondence $\hbar\omega = 3k_B T$ which gives the average phonon frequency $\omega$ of the phonons excited at temperature $T$, there are certainly not enough phonons excited at temperatures below $T_o \simeq 19$ K in our box to be able to reproduce the experimental curve correctly. In Figure 10, the departure between our simulations and experiments is actually seen at a temperature of the order of 20 K, in good agreement with this analysis.

To try to put this argument on more quantitative grounds, let us assume that the thermal conductivity is given by the usual formula [37],

$$\kappa = \frac{1}{3} C v \ell \tag{6}$$

where $C$ is the heat capacity per unit volume, $v$ and $\ell$ the velocity and mean free path of the phonons, respectively. When applying such a formula to

glasses one has to be careful because of localization effects. Obviously $v$ and $\ell$ are the characteristics of the "propagative" phonons, *i.e.*, those which really contribute to the transport phenomena. Consequently the heat capacity $C$ to be considered should be only due to the contribution of these phonons and therefore (according to other authors [20, 22]) should exhibit at low temperature the usual Debye behavior (the same as in crystals). If we assume also that the lack of phonons in our box, *i.e.*, a wrong value of $C$, is the essential cause for the underestimated calculated value of $\kappa$, a very simple and crude way to take care of this is to multiply our simulation results by a corrective factor $C_\infty/C_b$ which can be estimated by taking for $C_\infty$ and $C_b$ the heat capacities calculated in the Debye approximation for an infinite system and a finite cubic box of edge $L$, respectively. To calculate this temperature dependent factor we have used the standard formulae [37]

$$C_\infty = \frac{k_B}{2\pi^2}\left(\frac{1}{v_L^3}+\frac{2}{v_T^3}\right)\int_0^{\omega_D}\left(\frac{\hbar\omega/2k_BT}{\sinh(\hbar\omega/2k_BT)}\right)^2\omega^2 d\omega \tag{7}$$

$$C_b = \frac{k_B}{L^3}\sum_p\sum_{\vec{k}}\left(\frac{\hbar v_p k/2k_BT}{\sinh(\hbar v_p k/2k_BT)}\right)^2 \tag{8}$$

with $\omega_D^3 = (N/L^3)18\pi^2(1/v_L^3 + 2/v_T^3)^{-1}$. In the expression of $C_b$ the double sum runs over the three polarizations $p = L$, $T_1$, $T_2$ and over the first $N$ $\vec{k}$ vectors (quantized as indicated above) of lowest norm $k = |\vec{k}|$. For $N$ and $L$ we have taken the simulation values $N = 648$ and $L = 21.48$ Å and for the sound velocities the experimental values $v_L = 5.9 \times 10^5$ cm/s and $v_{T_1} = v_{T_2} = 3.75 \times 10^5$ cm/s [34]. When correcting our numerical data this way, we obtain the open squares represented in Figure 10 which turn out to be in very good agreement with the experimental results in the plateau region. Of course, our reasoning is very crude since it assumes that finite size corrections affect only the heat capacity contribution in the expression of $\kappa$ (Eq. (6)) and that the harmonic approximation holds for the propagative phonons in that temperature range, however we think that the agreement with the data cannot be fortuitous. It is unfortunate that we could not obtain more reliable results at temperatures lower than 8 K (due to the impossibility to reach the permanent regime). Anyway, after correction, these results would certainly give larger values for $\kappa$ than the experiments since it is known that, at very low temperatures, the propagative phonons start to be scattered on the quantum two level systems [20] and therefore

should have a lower mean free path than the one obtained in a classical calculation like the one performed here.

### D. Conclusion

In conclusion we have presented in this second part the results of an extensive classical molecular dynamics simulation aimed to determine the thermal conductivity in a model silica glass. This determination has been done directly inside the MD scheme with the use of the standard equations governing the macroscopic transport coefficients and no pre-conceived model has been assumed. Moreover it turns out that this method has considerable advantages (especially concerning the length of the simulations) compared to the standard methods usually implemented to calculate the transport coefficients [13]. The calculated values of the thermal conductivity are in good agreement with the experimental data at high temperature ($T > 20$ K) and by including finite size corrections in a simple way we are able to reproduce the plateau in the thermal conductivity around 10 K, which has been the topic of several interpretations in the literature [21]. The agreement between the calculated and the experimental values of the thermal conductivity is even more striking when taking into account the ultra-fast quenching rate used to generate our amorphous samples. This shows once more the good quality of the BKS potential which permits to reproduce the thermal anomalies of vitreous silica with no additional parameters.

Of course, our arguments on the finite size effects should be tested in the future by running larger samples. Nevertheless the simple phenomenological correction is so efficient that one can reasonably claim that the initial discrepancy between the calculated and experimental values of the thermal conductivity is indeed due to finite size effects and not to a weakness of the method. Therefore we believe that this technique is a good way to calculate the thermal properties of materials directly inside molecular dynamics simulations [38].



*Acknowledgments*

Most of the numerical calculations have been done on the IBM/SP2 computer at CNUSC (Centre National Universitaire Sud de Calcul), Montpellier. We would like to thank Claire Levelut and Jacques Pelous for very interesting comments.

It is our pleasure to thank Alain Fuchs for giving us the opportunity to be a part of the "Virtual Conference" MolSim'99 which was a new experience for us. Many thanks also to Sarah Dain for her technical help.

## *References*


[1] Elliott, S. R. (1991). "Origin of the first sharp diffraction peak in the structure factor of covalent glasses", *Phys. Rev. Lett.*, **67**, 711; Gaskell, P. H. and Wallis, D. J. (1996). "Medium-range order in silica, the canonical network glass", *Phys. Rev. Lett.*, **76**, 66; Fayos, R., Bermejo, F. J., Dawidowski, J., Fischer, H. E. and Gonzalez, M. A. (1996). "Direct Experimental Evidence of the Relationship between Intermediate-Range Order in Topologically Disordered Matter and Discernible Features in the Static Structure Factor", *Phys. Rev. Lett.*, **77**, 3823.

[2] Shuker, E. and Gammon, R. W. (1970). "Raman scattering selection rule breaking and the density of states in amorphous materials", *Phys. Rev. Lett.*, **25**, 223; Martin, A. and Brenig, W. (1974). "Model for Brillouin scattering in amorphous solids", *Phys. Status Solidi B*, **64**, 163; Akkermans, E. and Maynard, R. (1985). "Weak localization and anharmonicity of phonons", *Phys. Rev. B*, **32**, 7850; Buchenau, U., Zhou, H. M., Nücker, N., Gilroy, K. S. and Phillips, W. A. (1988). "Structural relaxation in vitreous silica", *Phys. Rev. Lett.*, **60**, 1318; Malinovsky, V. K., Novikov, V. N., Parshin, P. P., Sokolov, A. P. and Zemlyanov, M. G. (1990). "Universal form of the low-energy (2 to 10 meV) vibrational spectrum of glasses", *Europhys. Lett.*, **11**, 43; Novikov, V. N. and Sokolov, A. P. (1991). "A correlation between low-energy vibrational spectra and first sharp diffraction peak in chalcogenide glasses", *Solid State Commun.*, **77**, 243; Sokolov, A. P., Kisliuk, A., Soltwisch, M. and Quitmann, D. (1992). "Medium-range order in glasses: Comparison of Raman and diffraction measurements", *Phys. Rev. Lett.*, **69**, 1540; Börjesson, F. L., Hassan, A. K., Swenson, J., Torell, L. M. and Fontana, A. (1993). "Is there a correlation between the first sharp diffraction peak and the low frequency vibrational behavior of glasses?", *Phys. Rev. Lett.*, **70**, 1275; Gurevich, V. L., Parshin, D. A., Pelous, J. and Schober, H. R. (1993). "Theory of low-energy Raman scattering in glasses", *Phys. Rev. B*, **48**, 16318; Achibat, T., Boukenter, A. and Duval, E. (1993). "Correlation effects on raman scattering from low-energy vibrational modes in glasses. ii: experimental results", *J. Chem. Phys.*, **99**, 2046; Schirmacher, W. and Wagener, M. (1993). "Vibrational anomalies and phonon localization in glasses", *Solid State Commun.*, **86**, 597; Bermejo, F. J., Criado, A. and Martinez, J. L. (1994). "On the microscopic origin of the "boson" peak in glassy materials", *Phys. Lett. A*, 195, 236; Terki, F., Levelut, C., Boissier, M. and Pelous, J. (1996). "Low-frequency dynamics and medium-range order in vitreous silica", *Phys. Rev. B*, **53**, 2411.

[3] Jin, W., Vashishta, P., Kalia, R. K. and Rino, J. P. (1993). "Dynamic structure factor and vibrational properties of $SiO_2$ glass", *Phys. Rev. B*, **48**, 9359; Horbach, J., Kob, W. and Binder, K., "The dynamics of supercooled silica: acoustic modes and the boson peak", condmat/9710012.

[4] Taraskin, S. N. and Elliott, S. R. (1997). "Nature of vibrational excitations in vitreous silica", *Phys. Rev. B*, **55**, 117.

[5] Taraskin, S. N. and Elliott, S. R. (1997). "Phonons in vitreous silica: dispersion and localization", *Europhys. Lett.*, **39**, 37.

[6] Guillot, B. and Guissani, Y. (1997). "Boson peak and high frequency modes in amorphous silica", *Phys. Rev. Lett.*, **78**, 2401.

[7] Della Valle, R. G. and Andersen, H. C. (1992). "Molecular dynamics simulation of silica liquid and glass", *J. Chem. Phys.*, **97**, 2682.

[8] Woodcock, L. V., Angell, C. A. and Cheeseman, P. (1976). "Molecular dynamics studies of the vitreous state: simple ionic systems and silica", *J. Chem. Phys.*, **65**, 1565; Holender, J. M. and Morgan, G. J. (1991). "Molecular dynamics simulations of a large structure of amorphous Si and direct calculations of the structure factor", *J. Phys.: CM*, **3**, 1947; Servalli, G. and Colombo, L. (1993). "Simulation of the amorphous-silicon properties and their dependence on sample preparation", *Europhys. Lett.*, **22**, 107; Nakano, A., Bi, L., Kalia, R. K. and Vashishta, P. (1993). "Structural correlations in porous silica: Molecular dynamics simulation on a parallel computer", *Phys. Rev. Lett.*, **71**, 85; Sarnthein, J., Pasquarello, A. and Car, R. (1995). "Structural and electronic properties of liquid and amorphous $SiO_2$: an *ab initio* molecular dynamics study", *Phys. Rev. Lett.*, **74**, 4682.

[9] Vollmayr, K., Kob, W. and Binder, K. (1996). "Cooling-rate effects in amorphous silica: a computer-simulation study", *Phys. Rev. B*, **54**, 15808.

[10] van Beest, B. W. H., Kramer, G. J. and van Santen, R. A. (1990). "Force fields for silicas and aluminophosphates based on *ab initio* calculations", *Phys. Rev. Lett.*, **64**, 1955.
[11] Rustad, J. R., Yuen, D. A. and Spera, F. J. (1991). "Molecular dynamics of amorphous silica at very high pressures (135 gpa): thermodynamics and extraction of structures through analysis of voronoi polyhedra", *Phys. Rev. B*, **44**, 2108.
[12] Sadoc, J. F. and Mosseri, R., "La frustration Géométrique", Alea Collection, Eyrolles Ed., Saclay, France, 1997.
[13] Allen, M. P. and Tildesley, D. J. (1990). *Computer simulation of liquids*, Oxford University Press, New-York.
[14] Jund, P., Caprion, D. and Jullien, R. (1997). "Local investigation of the glass transition: molecular dynamics and voronoi tessellation", *Europhys. Lett.*, **37**, 547; Jund, P., Caprion, D. and Jullien, R. (1997). "The glass transition in a simple model glass: numerical simulations", *Mol. Sim.*, **20**, 3.
[15] Gellatly, B. J. and Finney, J. L. (1982). "Characterisation of models of multicomponent amorphous metals: the radical alternatice to the Voronoi polyhedron", *J. Non Cryst. Solids*, **50**, 313.
[16] Stillinger, F. H. and Weber, T. A. (1982). "Hidden structure in liquids", *Phys. Rev. A*, **25**, 978.
[17] Neuefeind, J. and Liss, K.-D. (1996). "Bond angle distribution in amorphous germania and silica", *Ber. Buns. Ges. Phys. Chem.*, **100**, 1341.
[18] Jullien, R., Jund, P., Caprion, D. and Quitmann, D. (1996). "Computer investigation of long-range correlations and local order in random packings of spheres", *Phys. Rev. E*, **54**, 6035.
[19] Bruckner, R. (1970). "Properties and structure of vitreous silica", *J. Non. Cryst. Solids*, **5**, 123; Zeller, R. C. and Pohl, R. O. (1971). "Thermal conductivity and specific heat of noncrystalline solids", *Phys. Rev. B*, **4**, 2029; Cahill, D. G. and Pohl, R. O. (1987). "Thermal conductivity of amorphous solids above the plateau", *Phys. Rev. B*, **35**, 4067.
[20] Anderson, P. W., Halperin, B. I. and Varma, C. M. (1972). "Anomalous low-temperature thermal properties of glasses and spin glasses", *Phil. Mag.*, **25**, 1; Phillips, W. A. (1972). "Tunneling states and the low-temperature thermal expansion of glasses", *J. Low Temp. Phys.*, **7**, 351.
[21] Graebner, J. E., Golding, B. and Allen, L. C. (1986). "Phonon localization in glasses", *Phys. Rev. B*, **34**, 5696; Yu, C. C. and Freeman, J. J. (1987). *Phys. Rev. B*, "Thermal conductivity and specific heat of glasses", **36**, 7620; Alexander, S., Entin-Wohlman, O. and Orbach, R. (1986). "Phonon-fracton anharmonic interactions: The thermal conductivity of amorphous materials", *Phys. Rev. B*, **34**, 2726.
[22] Karpov, V. G., Klinger, M. I. and Ignat'ev, F. N. (1983). "Theory of the low-temperature anomalies in the thermal properties of amorphous structures", *Sov. Phys. JETP*, **57**, 439; Ill'in, M. A., Karpov, V. G. and Parshin, D. A. (1987). "Parameters of soft atomic potentials in glasses", *Sov. Phys. JETP*, **65**, 165.
[23] Gil, L., Ramos, M. A., Bringer, A. and Buchenau, U. (1993). "Low-temperature specific heat and thermal conductivity of glasses", *Phys. Rev. Lett.*, **70**, 182.
[24] Tenenbaum, A., Ciccotti, G. and Gallico, R. (1982). "Stationary nonequilibrium states by molecular dynamics. Fourier's law", *Phys. Rev. A*, **25**, 2778; Mountain, R. D. and MacDonald, R. A. (1983). "Thermal conductivity of crystals: a molecular-dynamics study of heat flow in a two dimensional crystal", *Phys. Rev. B*, **28**, 3022.
[25] Maeda, A. and Munakata, T. (1995). "Lattice thermal conductivity *via* homogeneous nonequilibrium molecular dynamics", *Phys. Rev. E*, **52**, 234.
[26] Michalski, J. (1992). "Thermal conductivity of amorphous solids above the plateau: molecular-dynamics study", *Phys. Rev. B*, **45**, 7054.
[27] Oligschleger, C. and Schön, J. C. (1999). "Simulation of thermal conductivity and heat transport in solids", *Phys. Rev. B*, **59**, 4125.
[28] Ladd, A. J. C., Moran, B. and Hoover, W. G. (1986). "Lattice thermal conductivity: A comparison of molecular dynamics and anharmonic lattice dynamics", *Phys. Rev. B*, **34**, 5058.

[29] Allen, P. B. and Feldman, J. L. (1993). "Thermal conductivity of disordered harmonic solids", *Phys. Rev. B*, **48**, 12581; Feldman, J. L., Kluge, M. D., Allen, P. B. and Wooten, F. (1993). "Thermal conductivity and localization in glasses: numerical study of a model of amorphous silicon", *Phys. Rev. B*, **48**, 12589.
[30] Kaburati, H. and Machida, M. (1993). "Thermal conductivity in one-dimensional lattices of Fermi-Pasta-Ulam type", *Phys. Lett. A*, **181**(2), 85.
[31] Reif, F. (1965). In: *Fundamentals of statistical and thermal physics*, McGraw-Hill.
[32] Stephens, R. B. (1973). "Low-temperature specific heat and thermal conductivity of noncrystalline dielectric solids", *Phys. Rev. B*, **8**, 2896.
[33] Zarzycki, J. (1982). In: *Les verres et l'état vitreux*, Masson, Paris and references therein.
[34] Terki, F., Levelut, C., Boissier, M. and Pelous, J. (1996). "Low-frequency dynamics and medium-range order in vitreous silica", *Phys. Rev. B*, **53**, 2411.
[35] Winterling, G. (1975). "Very low frequency Raman scattering in vitreous silica", *Phys. Rev. B*, **12**, 2432; Galeener, F. L., Leadbetter, A. J. and Stringfellow, M. W. (1983). "Comparison of the neutron, Raman and infrared vibrational spectra of vitreous $SiO_2$, $GeO_2$ and $BeF_2$", *Phys. Rev. B*, **27**, 1052.
[36] We do find (like other authors [3]) an excess of modes at low frequencies compared with the Debye formula when diagonalizing the dynamical matrix. However the maximum of this excess of modes is located at a frequency of about 2 THz, *i.e.*, almost twice the experimental value. We think that this discrepancy is simply due to finite size effects: by reducing the lowest frequency $\omega_o$ one would shift this maximum excess of modes to lower frequencies.
[37] Kittel, C. (1970). In: *Introduction à la Physique de l'état solide*, Paris, Dunod.
[38] Jund, P. and Jullien, R. (1999). "Molecular Dynamics calculation of the thermal conductivity of vitreous silica", *Phys. Rev. B*, **59**, 13707.